

## **An Improved Methodology to Assess the Performance of Organic Corrosion Inhibitors**

J.M. Domínguez Olivo, D. Young, B. Brown, S. Nestic  
Institute for Corrosion and Multiphase Technology  
Department of Chemical & Biomolecular Engineering  
Ohio University  
Athens, OH 45701

### **ABSTRACT**

Qualification tests for determining the mitigation efficiency of surfactant-type organic corrosion inhibitors are conducted by performing corrosion rate measurements (typically with linear polarization resistance and/or weight loss method) at different inhibitor concentrations in simulated environmental conditions. The main assumption underlying this type of model is that the coverage of the metal surface by the corrosion inhibitor is equal to the corrosion mitigation efficiency. However, the present research highlights the effects that cause deficiencies in the interpretation of the “coverage” term by examining the mechanisms affected by the adsorption of an inhibitor. Employing quaternary ammonium-type of corrosion inhibitors, this study proposes a new methodology to assess the effectiveness of organic corrosion inhibitors by accounting for kinetic parameters of the electrochemical processes underlying CO<sub>2</sub> corrosion of mild steel.

### **INTRODUCTION**

Internal pipeline corrosion is one of the most challenging integrity problems relating to management of production and transportation assets in the oil and gas industry.<sup>1</sup> The associated risks have led to corrosion engineers developing both direct and indirect strategies to mitigate internal corrosion of pipelines. Injection of corrosion inhibitors is one of the most extensively applied and affordable methods to mitigate internal corrosion.<sup>1,2</sup>

A corrosion inhibitor is a chemical substance that can significantly reduce corrosion, in certain environments, when added in small concentrations (of the order of parts per million).<sup>3</sup> The oil and gas industry uses a variety of corrosion inhibitors,<sup>3</sup> with most of them being organic surfactant-type compounds such as amines and imidazolines, which primarily function by adsorbing on the

metal surface and forming some kind of “barrier” against corrosion.<sup>2,3</sup> It is said that this barrier with long hydrophobic hydrocarbon tail would restrict water coming into contact with the metal surface, thus inhibiting corrosion. Corrosion inhibitor molecules most commonly attach to the metal surface *via* their polar (hydrophilic) head group,<sup>4</sup> while the non-polar, hydrophobic alkyl tail of the inhibitor is assumed to be oriented away from the surface.<sup>4</sup> Regarding the effect of the alkyl tail length of the corrosion inhibitor, there have been studies relating the alkyl tail with the mitigation efficiency of the corrosion inhibitors; in these studies, corrosion inhibition efficiency and/or changes in the double layer capacitances were measured.<sup>4-8</sup> Measurements were integrated into mathematical models based upon adsorption isotherms assuming that the coverage of the inhibitor on the metal surface ( $\theta$ ) is proportional to the corrosion mitigation efficiency, as is common practice.<sup>3,9-11</sup> Nonetheless, studies equating surface coverage and efficiency of corrosion inhibitors can be biased. The methods utilized may lead to wrong conclusions due to misinterpretation of the results. Often, critical mechanistic considerations of the electrochemical nature of acidic corrosion of metals is disregarded in the analysis. The limiting current of the hydrogen evolution is, perhaps, the most important and yet overlooked parameter in the analysis of corrosion inhibition. A second mistake often made is in the interpretation of the Tafel slopes associated with the dissolution of metals and hydrogen evolution in the presence of inhibitors. Given their importance, the current research effort will analyze the effects of the limiting current and the Tafel slopes in the interpretation of the results.

### **Limiting Current Effects: Partially blocked Electrode Kinetics and Microelectrode Array Hypothesis**

The blockage model<sup>2</sup> associates the decrease of active surface area with the reduction of corrosion rates. From this point of view, the corrosion current density diminishes because a smaller active area produces the total current pertained to corrosion. However, this perceived diminishing the active surface area does not explain some experimental observations.

A hypothetical scenario illustrates the idea: a 1 cm<sup>2</sup> steel sample undergoes acidic aqueous corrosion. The total corrosion current is measured with LPR: 0.1 mA. Therefore, the corrosion current density is equal to 0.1 mA/cm<sup>2</sup> (corresponding to ~1 mm/year in the case of mild steel). An organic corrosion inhibitor is injected at the beginning of a new experiment. After a few hours, the measured corrosion total current stabilizes at 0.01 mA. To obtain the current density, the total current is divided by the total initial area of the electrode, obtaining a corrosion current density of 0.01 mA/cm<sup>2</sup> and a corrosion rate of 0.1 mm/year. The efficiency is calculated to be 90%. Under the blockage model, the result implies that the active surface area of the metal was diminished down to 10% of the original surface area. In other words, the total corrosion current obtained is equivalent to the total corrosion current of a 0.1 cm<sup>2</sup> electrode. Following the logic of the blockage model, if there is a decrease in the active surface area, all electrochemical reactions associated with the corrosion of mild steel would be affected (Figure 1). The plot shows two hypothetical potentiodynamic sweeps for the described electrodes with different surface areas.

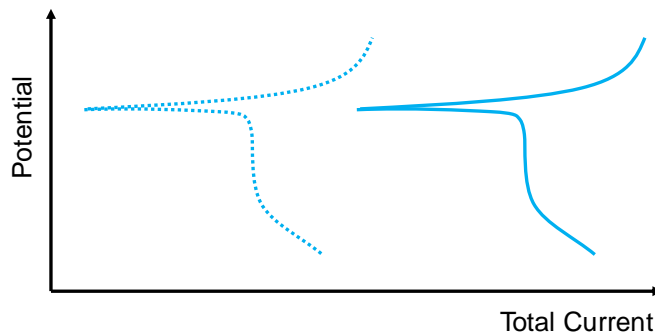


**Figure 1. Hypothetical potentiodynamic sweeps for two electrodes with different active surface areas under the same conditions.**

When the total current is divided by the true active area of the corresponding electrode to obtain current density, the curves should overlap. Figure 2 shows that experimental potentiodynamic polarization curves in the absence and presence of corrosion inhibitors do not behave as two electrodes with different areas. The main difference lies in the limiting current, which is not affected by the presence of two types of organic corrosion inhibitors (imidazoline and quaternary ammonium-type, respectively).

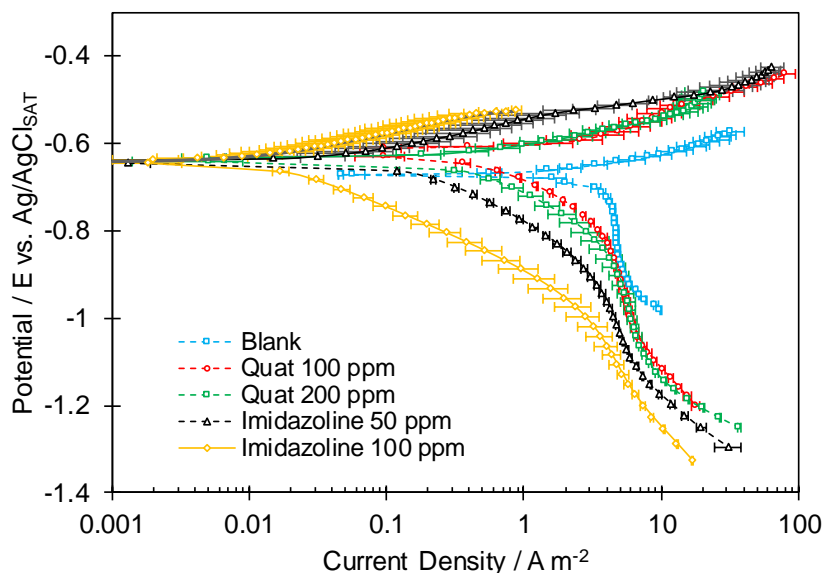


**Figure 2. Potentiodynamic polarization curves of an X65 steel working electrode 1000 RPM RCE at 30 °C, 0.96 bar CO<sub>2</sub>, in the presence of a quaternary ammonium-type of corrosion inhibitor and imidazoline-type of corrosion inhibitors at different concentrations. Limiting currents are unaffected by the presence of the inhibitors in all cases. Error bars: maximum and minimum currents obtained at selected potentials.**

One strong argument to sustain the blockage model in conjunction with the fact that the limiting currents are not affected can be the partially blocked electrode kinetic theory described by Gileadi

*et al.*<sup>12</sup> Specifically, the case for electrodes modified by a blocking material. To study the effect of electrode distribution, the author developed microelectrode arrays embedded in an insulator material as shown in Figure 3.

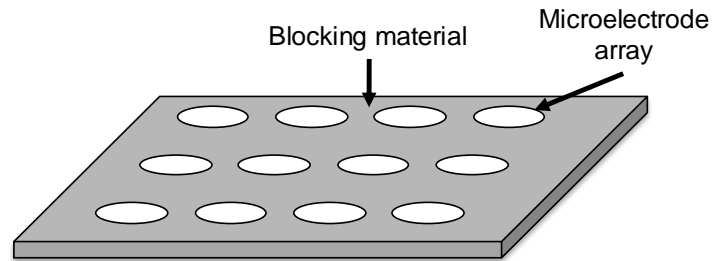


**Figure 3. Microarray electrodes embedded in an insulating material. This array represents a partially blocked electrode.**

From the blockage model of inhibition, the effect of corrosion inhibitors on the metal surface can be modeled with microelectrode arrays. Each microelectrode corresponds to the active surface area of the electrode. The inhibitor is represented by the insulating material.

Many researchers have performed cyclic potentiodynamic polarization, cyclic polarization, and polarography to demonstrate that the blocking material diminishes the rate of the processes under charge transfer regions as a linear function of the blocked surface<sup>12-16</sup>. However, the diffusion limiting currents change depending on the distribution of the blocked material. Such a distribution can be stated by two possible scenarios: the individual non-linear concentration profile (Figure 4) and the case for overlapping non-linear diffusion layers (Figure 5)<sup>13</sup>.

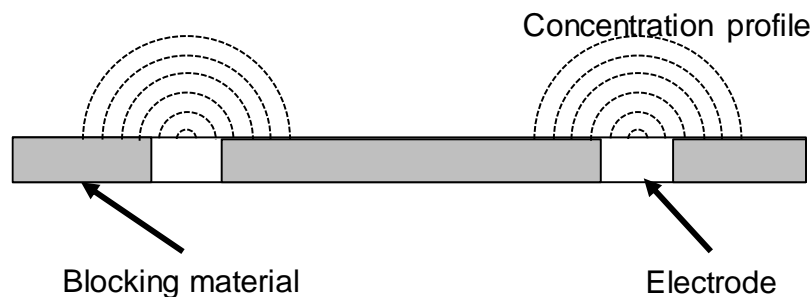


**Figure 4. Partially blocked electrode: the case for individual non-linear diffusion layers.**

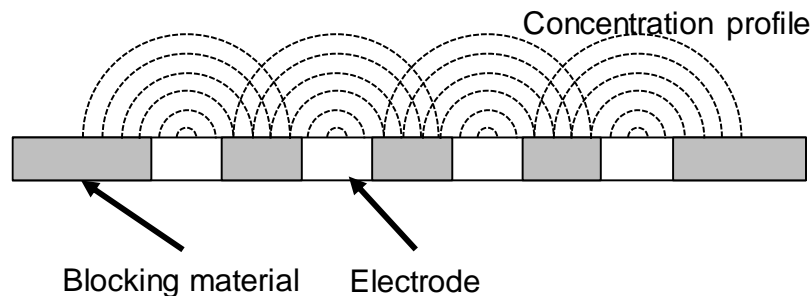


**Figure 5. Partially blocked electrode: the case for overlapping non-linear diffusion layers**

When the diffusion profiles of the microelectrodes do not overlap, the limiting current diminishes proportionally to the active surface area. In the case of overlapping, the limiting currents are the same as in a bare electrode. Subsequently, assuming that a corrosion inhibitor would adsorb in such a way that the diffusion profiles overlap can explain why the limiting current is unchanged.

However, Amatore *et al.*,<sup>16–18</sup> demonstrated that the limiting current diminishes regardless of the active surface area distribution in partially blocked microelectrodes ensembles with high coverage (*i.e.*,  $\theta > 0.9$ ). The distance between the active sites at high coverage is such that the concentration profiles do not overlap, resembling the scenario depicted in Figure 4.

For the case of corrosion inhibition, there are corrosion inhibitors with efficiencies higher than 90% (and therefore  $\theta > 0.90$  under the blockage model). For instance, 100 ppm of an imidazoline-type of corrosion inhibitor would imply that the limiting current is affected by the coverage of the inhibitor. Nonetheless, Figure 2 showed that it is not the case.

### **Blockage Model and Activation Energy**

The activation energy for a reaction is a measurement that indicates the energy that needs to be supplied so the reaction can proceed. In the case of electrochemical dissolution of metal, the reaction involves charged ionic species moving across an electric field generated by a double layer structure at the metal surface. Therefore, in a general case, one needs to consider both the chemical and the electrical component of the activation energy.<sup>19–21</sup> Figure 6 represents a schematic illustrated textbook example<sup>19</sup> of the oxidative dissolution of metal and the associated free energy diagram, showing the total activation energy for this reaction as being composed of two parts; a chemical component and an electrical component:

$$\Delta\tilde{G}_M^* = \Delta G_M^* + \beta F \Delta\Phi \quad (1)$$

where  $\Delta\tilde{G}_M^*$  is the total activation free energy,  $\Delta G_M^*$  is the chemical component of the activation energy of the electrochemical process,  $\beta$  is a symmetry factor,  $F$  is the Faraday constant and  $\Delta\Phi$  is the potential drop across the double layer.

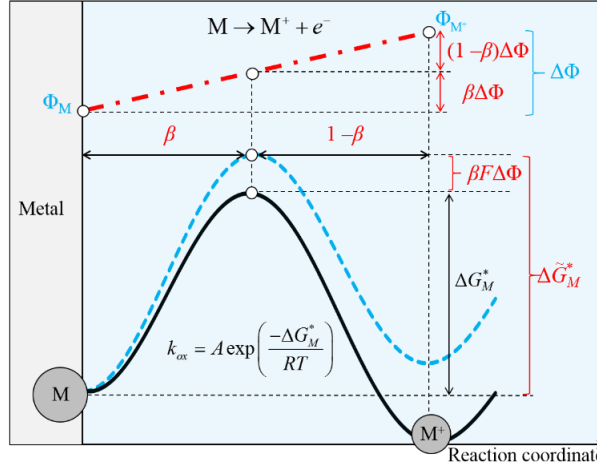


**Figure 6. Free energy diagram for an anodic reaction ( $M \rightarrow M^+ + e^-$ ). The total activation energy of this reaction is divided into a chemical component (black curve) and an electrical component (dash point red line). The combination of the two is shown as a dash blue curve. Adapted from Bockris, *et al.* <sup>19</sup>**

The anodic dissolution process is then accelerated and retarded according to the change in the potential drop or a change in the chemical component of the activation energy equation. Under this premise, one is led to think that the presence of a corrosion inhibitor would increase the activation energy of the electrochemical reactions, so the anodic dissolution proceeds at a slower rate.

However, the formulation of the blockage model implies that the activation energy of the electrochemical reactions underlying corrosion is unchanged. To explain the statement, one can express the rate of the abovementioned anodic dissolution at the reversible potential as:

$$i = Fk_M \exp\left(-\frac{\Delta G_M^*}{RT}\right) \exp\left(-\frac{\beta F \Delta \Phi}{RT}\right) \quad (2)$$

Assuming that the exchange current density in the presence of a corrosion inhibitor diminishes only due to the diminution of the active surface area (as per the blockage model), the exchange current density in the presence of a corrosion inhibitor,  $(i_0)_{inh}$ , can be expressed as :

$$(i_0)_{inh} = (1 - \theta)i_0 = (1 - \theta)Fk_M \exp\left(-\frac{\Delta G_M^*}{RT}\right) \exp\left(-\frac{\beta F E_{rev}}{RT}\right) \quad (3)$$

Where  $\theta$  is the coverage of the inhibitor, and  $E_{rev}$  is the reversible potential given by the Nernst equation.

Given the following textbook relationship<sup>22</sup>:

$$nFE_{rev}^0 = -\Delta G^0 = T\Delta S^0 - \Delta H^0 \quad (4)$$

For a single step, electrochemical reaction,  $n = 1$ . Expanding the Gibbs energy of activation into the enthalpy and entropy components, the exchange current density in the presence of a corrosion inhibitor is then expressed as:

$$(i_0)_{inh} = (1 - \theta) F k_M \exp\left(\frac{\Delta H_M^* - T \Delta S_M^*}{RT}\right) \exp\left(-\frac{\beta(\Delta H^0 - T \Delta S^0)}{RT}\right) \quad (5)$$

As the formulation is written in terms of equilibrium conditions, one can apply the formal thermodynamic definition of activation energy:

$$-R \left( \frac{\partial \ln |k_{eq}|}{\partial (1/T)} \right) = E_A \quad (6)$$

For this case, letting  $(i_0)_{inh} = k_{eq}$ , the partial derivative of the natural logarithm of the exchange current density in the presence of an inhibitor with respect to the inverse of the temperature is expressed as:

$$-R \left( \frac{\partial \ln |(i_0)_{inh}|}{\partial (1/T)} \right) = (E_A)_{inh} = \Delta H_M^* - \beta \Delta H^0 \quad (7)$$

The result of Equation (7) would be the same if the coverage term  $(1-\theta)$  is not present in Equation (5). The simple blockage model thermodynamically implies that the activation energy associated with the anodic dissolution of metal is independent of the active surface area of the electrode  $(1-\theta)$ . This result suggests that the presence of a corrosion inhibitor would not change the activation energy of the anodic dissolution of metal if the blockage is the only effect associated with the adsorption of the corrosion inhibitor. Notwithstanding, this result is in odds with experimental observations from various research that have shown that the presence of a corrosion inhibitor indeed changed the activation energy of a metal dissolution process<sup>23-26</sup>.

Given the experimental observations and the conclusions from other scientific fields analogous to the corrosion inhibition phenomenon, the assumption that coverage is equal to efficiency seems insufficient to describe the phenomenon of corrosion inhibition completely. That is the motivation of this research: to propose a more comprehensive methodology to assess the effect of corrosion inhibitor that accounts for changes in the electrochemical reactions governing the acidic corrosion of mild steel due to a corrosion inhibitor adsorption.

## METHODOLOGY

A three-electrode glass cell setup was used to perform corrosion and corrosion mitigation experiments at 1 bar, pH 4.0 and 30, 35, 40 and 45 °C with a 1 wt. % NaCl electrolyte; a UNS K03014 API 5L X65 steel (Fe 97.7, C 0.13, Mn 1.16, Mo 0.16 wt.%) rotating cylinder electrode (RCE) at 1000 rpm was used as the working electrode. A platinum covered titanium mesh was used as a counter electrode and an Ag/AgCl (KCl saturated) electrode was used as the reference. Figure 7 shows an illustration of the apparatus. CO<sub>2</sub> gas was used for purging of the system and the solution pH was adjusted and maintained at pH 4.0±0.1 during each experiment. Linear polarization resistance (LPR) measurements were taken to obtain the charge transfer resistance by polarizing the working electrode from -5 mV to +5 mV measured from the corrosion potential; instantaneous corrosion rates were then estimated using a  $B$  value of 26 mV/decade. Corrosion

inhibitors were tested at the so called “surface saturation concentration”, which is the minimum concentration that yielded the maximum efficiency (lowest corrosion rate) for a given corrosion inhibitor. Each experiment was performed three times. A summary of the experimental conditions is given in Table 1.

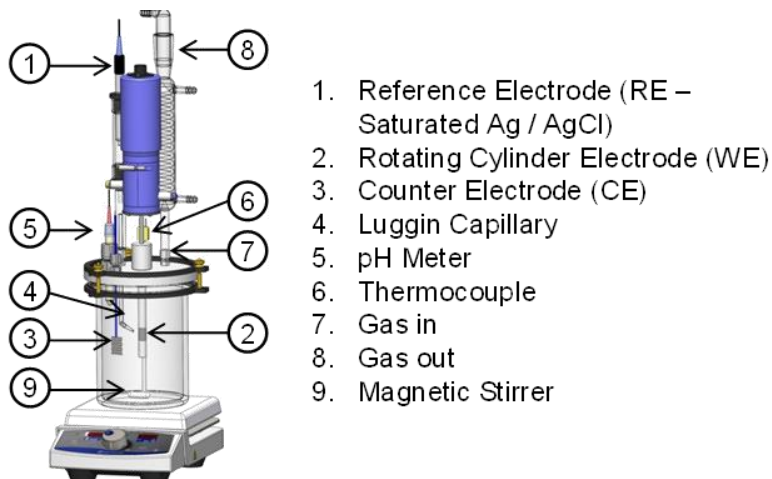


**Figure 7: Three electrode set up used to perform experiments.<sup>(1)</sup>**

**Table 1. Experimental Conditions**

Description	Parameters
Test material	API 5L X65
Working solution	1 wt.% NaCl
Spurge gas	CO <sub>2</sub>
Temperature / °C	30, 35, 40, 45
pH	4.0 ± 0.1
Corrosion inhibitors	None (baseline), Model Compounds: Q-C4 (50, 100, 150, 200 ppm) Q-C8 (50, 100, 150, 200 ppm) Q-C12 (50, 100, 150, 200 ppm) Q-C16 (50, 100, 150, 200 ppm)
Test duration	2-12 hours (stabilization of corrosion rate)
Measurement methods	LPR, EIS, potentiodynamic polarization

<sup>(1)</sup> Image courtesy of Cody Shafer, ICMT, Ohio University.

## RESULTS AND DISCUSSION

### Effect of corrosion inhibitor on the electrochemical reactions

The key overall electrochemical reactions associated with the corrosion of mild steel in CO<sub>2</sub> saturated aqueous environments are the anodic dissolution of iron:



And the hydrogen evolution reaction:



These are multistep reactions and are fully addressed in the context of acidic CO<sub>2</sub> corrosion by Kahyarian, *et al.*<sup>27</sup> For the case of the hydrogen evolution in acidic aqueous environments, the Volmer reaction is assumed to be the rate-determining step (rds):



The Volmer reaction as the rds yields Tafel slopes close to 2RT/F (120 mV/decade).

In a similar scenario with corrosion inhibitors, Conway and Gileadi<sup>28</sup> have discussed the implication of having an electrode with high total coverage, defining the rate of the Volmer equation as:

$$i_{\text{H}^{+}} = k_{\text{H}^{+}} C_{\text{H}^{+}} (1 - \theta_T) \exp \left[ -\frac{\Delta G_{\text{H}^{+}}^{*} + f(\theta_T)}{RT} \right] \exp \left[ -\frac{\beta F \Delta \Phi}{RT} \right] \quad (11)$$

Where:  $\theta_T$  is the total coverage of the electrode,  $\Delta G_{\text{H}^{+}}^{*}$  is the chemical component of the activation energy of the reaction, and  $f(\theta_T)$  is a function that determines the variation of the activation energy with respect to the total coverage.

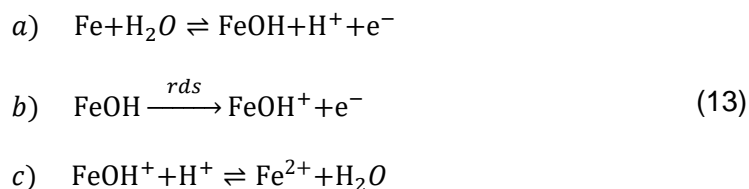
Conway, Gileadi and Thomas<sup>28,29</sup> discussed that the Volmer reaction has a coverage independent activation energy for  $\theta_T < 0.8$ . For coverages higher than 0.8, the energy of adsorption of the intermediate  $\text{H}_{ads}$  increases as per Frumkin kinetics<sup>29</sup>:

$$\Delta G_{ads} = \Delta G_{ads}^0 + r\theta_T \quad (12)$$

Where  $r$  is a constant relating to the increase of the standard adsorption energy at zero coverage ( $\Delta G_{ads}^0$ ) and the total coverage of the electrode.

The increase in the adsorption energy stabilizes the adsorbed hydrogen intermediate, making the recombination of the hydrogen (Tafel reaction) the rate-determining step<sup>28,29</sup>. Such a situation changes the Tafel slope from 2RT/F to 3RT/F (~180 mV/decade at 25 °C). A similar effect on the Tafel slope was reported by Gileadi<sup>30</sup> in the presence of organic molecules adsorbed on electrodes at high coverages. The author argued that the “electrosorption” of organic molecules (the replacement reaction of  $n$  water molecules by an organic molecule at the electrode surface) diminished the sites where the intermediate hydrogen adsorbed can recombine, making it the rate-determining step<sup>30</sup>.

In the case of the iron dissolution, the Bockris-Drazic-Despic (BDD) mechanism<sup>31</sup> is widely accepted to occur under the acidic dissolution of iron<sup>27,32</sup>, where the rate-determining step is the oxidation of the adsorbed intermediate FeOH:



Following the derivation previously described for hydrogen evolution, the rate of the reaction (13) as a function of the total coverage can be expressed as<sup>28,30</sup>:

$$i_{\text{FeOH}} = k_{\text{FeOH}} \theta_{\text{FeOH}} (1 - \theta_T) \exp \left[ -\frac{\Delta G_{\text{FeOH}}^* + f(\theta_T)}{RT} \right] \exp \left[ -\frac{\alpha F \Delta \Phi}{RT} \right] \tag{14}$$

Equation (14) implies that the coverage may affect the reaction by diminishing the space where the intermediate can form as well as modifying the chemical component of the activation energy associated with the reaction. Therefore, if the coverage is high, the low availability of water for the reaction (13) would make it the rate-determining step, changing the Tafel slope from  $3RT/2F$  (~40 mV/decade at 25 °C) to  $2RT/F$  (~120 mV/decade at 25 °C)<sup>28</sup>.

For the case of the quaternary ammonium model compounds studied in this work, the kinetics parameters were obtained by using the Tafel approximation as pointed by Nordsveen, *et al.*<sup>32</sup>, and more recently by Kahyarian, *et al.*<sup>27</sup>:

$$i = i_0 10^{\pm \frac{\eta}{b}} \tag{15}$$

In the case of the hydrogen ion reduction, a mathematical approximation was utilized to account for the limiting current<sup>27,32</sup>:

$$\frac{1}{i^c} = \frac{1}{i_{ct}^c} + \frac{1}{i_{lim}} \tag{16}$$

Figure 8 shows the mathematical fit for obtaining the kinetics parameters (Tafel slope, limiting current and exchange current density). The fit parameters for all the inhibitors found at 30°C are summarized in Table 2.

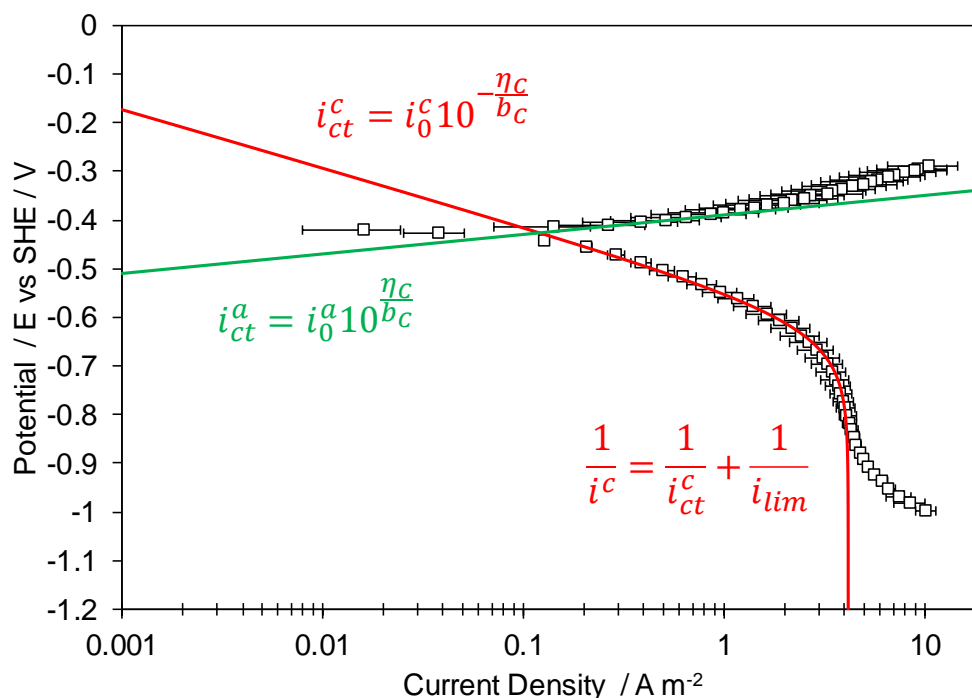


**Figure 8. Square markers: potentiodynamic sweep for a 0.96 bar CO<sub>2</sub>, pH 4, 30 °C, 1000 RPM RCE X65 steel with 50 ppm of Q-C16. Error bars: maximum and minimum current density at selected potentials from three different experiments. Green solid line: anodic current density model. Red solid line: cathodic current density model.**

**Table 2. Estimated kinetic parameters in the presence of corrosion inhibitors.**

System	Tafel Slope (mV/ Decade)		Exchange current density (A/m <sup>2</sup> )		i <sub>lim</sub> (A/m <sup>2</sup> )
	Anodic	Cathodic	Anodic	Cathodic	
Blank (CO <sub>2</sub> )	40-60	120-130	0.06	0.04	3.1-4.2
CO <sub>2</sub> + Q-C4	40-50	120-130	0.03	0.02	3.2-4.2
CO <sub>2</sub> + Q-C8	40-50	120-130	0.022	0.015	3.1-3.8
CO <sub>2</sub> + Q-C12	40-60	120-140	0.01	0.007	2.9-4.2
CO <sub>2</sub> + Q-C16	40-60	120-140	0.003	0.002	2.8-4.2

The facts that the Tafel slope of 120 mV/decade at high corrosion mitigation efficiency (~95%) and that the limiting currents are unchanged by the presence of the corrosion inhibitors suggest that the inhibitor mainly acts by changing the chemical component of the activation energy as shown by Equation (11)(10) and Equation (14). Such a statement is in good agreement with previous experimental results showing an increase in the activation energy of the electrochemical process underlying corrosion<sup>33</sup>.

## CONCLUSIONS

- A thermodynamic and kinetic analysis of corrosion based on metal dissolution theory was proposed to explain the effect of corrosion inhibitor model compounds adsorbed on steel.
- The Tafel slopes were not significantly affected by the presence of the corrosion inhibitors, suggesting that the mechanism of the hydrogen evolution and iron dissolution were not affected by the presence of the organic corrosion inhibitor model compounds.

## ACKNOWLEDGMENTS

The authors would like to thank the following companies for their financial support: Anadarko, Baker Hughes, BP, Chevron, CNOOC, ConocoPhillips, DNV GL, ExxonMobil, M-I SWACO (Schlumberger), Multi-Chem (Halliburton), Occidental Oil Company, Pioneer Natural Resources, Saudi Aramco, Shell Global Solutions, SINOPEC (China Petroleum), and TOTAL.

## REFERENCES

1. Jones, D.A., *Principles and Prevention of Corrosion* (New York: MacMillan, 1996).
2. McCafferty, E., *Introduction to Corrosion Science*, Springer (2010).
3. Sastri, V.S., *Green Corrosion Inhibitors*, 2nd ed. (Hoboken, NJ, USA: John Wiley & Sons, 2011).
4. Edwards, A., C. Osborne, S. Webster, D. Klenerman, M. Joseph, P. Ostovar, and M. Doyle, *Corros. Sci.* 36 (1994): pp. 315–325.
5. Palomar-Pardavé, M., M. Romero-Romo, H. Herrera-Hernández, M.A. Abreu-Quijano, N. V. Likhanova, J. Uruchurtu, and J.M. Juárez-García, *Corros. Sci.* 54 (2012): pp. 231–243.
6. Asefi, D., M. Arami, A.A. Sarabi, and N.M. Mahmoodi, *Corros. Sci.* 51 (2009): pp. 1817–1821.
7. Ali, S.A., A.M. El-Shareef, R.F. Al-Ghamdi, and M.T. Saeed, *Corros. Sci.* 47 (2005): pp. 2659–2678.
8. McCafferty, E., and N. Hackerman, *J. Electrochem. Soc.* 119 (1972): p. 146.
9. Vracar, L.M., and D. Drazic, *Corros. Sci.* 44 (2002): pp. 1669–1680.
10. Lorenz, W.J., and F. Mansfeld, *Electrochim. Acta* 31 (1985): pp. 467–476.
11. Cao, C., *Corros. Sci.* 38 (1996): pp. 2073–2082.
12. Reller, H., E. Kirowa-Eisner, and E. Gileadi, *J. Electroanal. Chem.* 138 (1982): pp. 65–77.
13. Davies, T.J., C.E. Banks, and R.G. Compton, *J. Solid State Electrochem.* 9 (2005): pp. 797–808.
14. Davies, T.J., B. a. Brookes, and R.G. Compton, *J. Electroanal. Chem.* 566 (2004): pp. 193–216.
15. Daniele, S., I. Lavagnini, M.A. Baldo, and F. Magno, *J. Electroanal. Chem.* 404 (1996): pp. 105–111.

16. Amatore, C., M.R. Deakin, and R.M. Wightman, *J. Electroanal. Chem.* 220 (1987): pp. 49–63.
17. Amatore, C., J.M. Savéant, and D. Tessier, *J. Electroanal. Chem.* 147 (1983): pp. 39–51.
18. Amatore, C., J.M. Savéant, and D. Tessier, *J. Electroanal. Chem. Interfacial Electrochem.* 147 (1983): pp. 39–51.
19. Bockris, J.O., A.K.N. Reddy, and M. Gamboa-Aldeco, *Ann. N. Y. Acad. Sci.* 1228 (2001): pp. 1–817.
20. Bockris, J.O., and Z. Nagy, “Symmetry Factor and Transfer Coefficient. A Source of Confusion in Electrode Kinetics,” *Journal of Chemical Education* (1973).
21. Crundwell, F.K., *Hydrometallurgy* 139 (2013): pp. 132–148.
22. Bard, A., and L. Faulkner, *Electrochemical Methods Fundamentals and Applications*, Electrochemical Methods, 2nd ed. (New York: John Wiley & Sons, Inc., 2001).
23. Desimone, M.P., G. Gordillo, and S.N. Simison, *Corros. Sci.* 53 (2011): pp. 4033–4043.
24. Zhang, Q.B., and Y.X. Hua, *Electrochim. Acta* (2009).
25. Sankarapavinasam, S., F. Pushpanaden, and M.F. Ahmed, *Corros. Sci.* (1991).
26. Beszeda, I., D.L. Beke, and Y. Kaganovskii, *Surf. Sci.* 569 (2004): pp. 5–11.
27. Kahyarian, A., M. Singer, and S. Nestic, *J. Nat. Gas Sci. Eng.* 29 (2016): pp. 530–549.
28. Conway, B.E., and E. Gileadi, *Trans. Faraday Soc.* 58 (1962): pp. 2493–2509.
29. Thomas, J.G.N., *Trans. Faraday Soc.* 57 (1961): pp. 1603–1611.
30. Gileadi, E., *Phys. Chem. Liq.* 7 (1978): pp. 239–242.
31. Bockris, J.O., D. Drazic, and A. Despic, *Electrochim. Acta* 4 (1961): pp. 325–361.
32. Nordsveen, M., and S. Nešić, *Corrosion* 59 (2003): pp. 443–456.
33. Dominguez Olivo, J.M., “Effect of Corrosion Inhibitor Alkyl Tail Length on the Electrochemical Process Underlying CO<sub>2</sub> Corrosion of Mild Steel,” in *Corros. 2018* (2018).